

TAGUCHI OPTIMISATION ON EFFECT OF WATER ENVIRONMENT IN JOINING DISSIMILAR AL5083 AND AL6061-T6 ALUMINIUM ALLOY USING FRICTION STIR WELDING

Muhammed Zakariya Hasnol^{1,*}, Mohd Faridh Ahmad Zaharuddin^{1,*}, Safian Sharif¹ and Sehu²

¹ School of Mechanical Engineering, Faculty of Engineering,
Universiti Teknologi Malaysia,
81310 UTM Johor Bahru, Johor, Malaysia

² Department of Mechanical Engineering
Universiti Hanyang, 17 Haengdang-dong, Seongdong-gu. Seoul 133-791,
Korea

*Corresponding email: faridh@mail.fkm.utm.my

Article history

Received
12th December 2021
Revised
8th June 2022
Accepted
8th June 2022
Published
22nd June 2022

ABSTRACT

Water cooling has the potential to improve the mechanical qualities of weldment joints in butt welding configurations. However, the joining procedure on such a configuration faces a challenging defect-free joining issue with the standard approach. This project investigates the effect of welding conditions on the joint quality using three different tool pin profiles (cylindrical straight, cylindrical threaded and tapered cylinder) during dissimilar underwater friction stir welding of a 6 mm thick plate. An experimental method following Taguchi parametric design is carried out to optimise the technique on hardness and microstructure at the weld nugget. ANOVA is used to assess the effect of each process parameter, namely tool pin profiles, welding speed, welding speed, and hardness responses. The water environment approach lowers thermal flow by maintaining consistent temperature from tool pin profiles. The combination of ongoing process parameters and fast-cooling rate induced heat input improves the welded joint's mechanical characteristics and microstructural grain. The experiment revealed the appropriate process parameters of 900 rpm, 60 mm/min, and tapered cylinder pin profile. Consequently, water-cooling significantly contributes to welded joints' mechanical properties and microstructure at the optimal parameter level, resulting in improved strength performance.

Keywords: *Underwater friction stir welding, dissimilar material, aluminium alloy, Taguchi*

© 2022 Penerbit UTM Press. All rights reserved

1.0 INTRODUCTION

Friction stir welding (FSW) is a solid-state joint technology that produces high-quality, low-distortion, high-strength butt or lap connections in a variety of material thicknesses and lengths [1] [2]. Taguchi parametric design is an excellent approach for identifying relevant parameters and responses at any experimental method of each process. An optimisation of friction stirs welding parameter, which can correlate during joining dissimilar materials, involves mechanical properties using the Taguchi method [3]. The optimal process parameters are determined to optimise weld joint mechanical properties. The experiment conducted the statistical analysis of variance (ANOVA) to examine the

appropriate range of process factors and their effects on weldment joint strength that are statistically significant [4]. The ANOVA techniques on the weld parameters are highly influential and have relative effects on responses [5]. In this study, the experimental method was optimised based on Taguchi and ANOVA in which the performance characteristics of process parameters with respect to output response of AA5083 and AA6061-T6.

The tool consists of a pin and a shoulder, more significant in diameter than the pin. Heat is generated when the shoulder contacts the base material [6]. Various pin tools include single-cylinder, threaded cylinders, conical cylinders, and enclosed cylindrical threads. The tiny grain structure of FSW leads to the production of new grains in the agitated area due to the extreme deformation of plastic, resulting in considerable microstructure growth [7]. Precipitate dissolving or coarsening causes material softening, which leads to lower mechanical performance and joint properties [8]. Water used as external cooling in several solid-state joining methods to improve joint performance [9]. Water-cooling has been examined as a means of cooling samples during the welding process due to its rapid circulation and strong heat absorption. As the pin rotation speed increases, the speed of the shoulder increases, creating tremendous heat in the connecting area, which contributes to approximately 95% of the total shoulder heat created [10]. The water environment during FSW may be used between weldment joints of aluminium alloy (AA5083) and magnesium alloy (AZ31), resulting in a cleaner interface and 250C less peak temperature material intermixing [11]. Furthermore, when the microstructure is investigated, water cooling can offer a more refined grain than air cooling [12].

It was proven on the FSW of Al-alloy at various rotational speeds (700,800, 900 rpm) and transverse speeds (40, 60, 80 mm/min) that there is an accurate combination of the weldment formed by strength and hardness in metallurgical bonding [113]. However, the rotating tool speed and tool pin shape significantly impacted the strength and microstructure of FSW AA5083-H11 and AA6351-T6 Al-alloys [14]. As a result, even though the joint design was meant to analyse process elements' effect on weldment quality, the solid-state nature was influenced by tool design, material flow, and welding conditions. The grades of alloying element addition on their samples may also improve joints' thermal stability structural features [15]. Structural metallic alloys' quality and microstructure properties exhibit different cooling rate techniques [16]. Mechanical testing on FSW AA5083- and AA6111-T4 Al alloys demonstrated that the alloy had the same strength as the welded zone AA6111 alloy's base material (B.M.) [17]. However, the weld zone in the AA5083-H18 alloy is notably softer than the base material. Because of porosity, the softening zone is related to the heat generated by the FSW process, and the kissing bond was formed when the welding speed rose while the position was on the retreating side [18]. Mechanical testing was performed on the micro-hardness distribution of the FSW of high zinc brass at three depths from the top pin profile. The association between temperature and hardness was established.

In addition, heat. Furthermore, due to frictional forces and material flow stirring, heat production significantly influenced the hardness scale for varied tool pin profiles during FSW of brasses [19]. Some references may be found in the lowest hardness under the pin across stir zone areas, farther in the thermo-mechanically affected zone (TMAZ) regions, where defect-free was reported [20]. FSW gave the lowest hardness beneath the pin across the stir zone while combining non-weldable AA7075 and weldable AA6061 aluminium alloy sheets stir zone. Reprecipitation enhances hardness due to solid solutions in welded seams during quick cooling for natural ageing on the retreating side [21].

This welding approach is ideally suited for alloys prone to overheating during the welding process, and it is commonly used for aluminium alloys [22]. The goal of this UFSW technology was to decrease heat consumption by reducing the detrimental effect material of FSW joints, which may improve the final joint's hardness and mechanical properties [23]. The joint strength was determined by the minimum hardness values in the

HAZ and increasing the rotation speed away from the welding core [24]. As a result, underwater FSW covers many marine and offshore applications. AA5083 and AA6061-T6, for example, are often used in the fabrication and maintenance of shipyards, warships, oil and fuel tanks, and other offshore structures.

2.0 MATERIAL AND EXPERIMENTAL PROCEDURES

The FSW process was carried out on these sheet metals as main materials, AA5083 and AA6061-T6, with (150mm×65mm×6mm). The vertical milling machine used in the experiment, as shown in Figure 1, is a Lagun vertical milling machine outfitted with a rig water container. The operating ranges of the two variables, rotation speed and welding speed, are analysed to define the correct material flow.

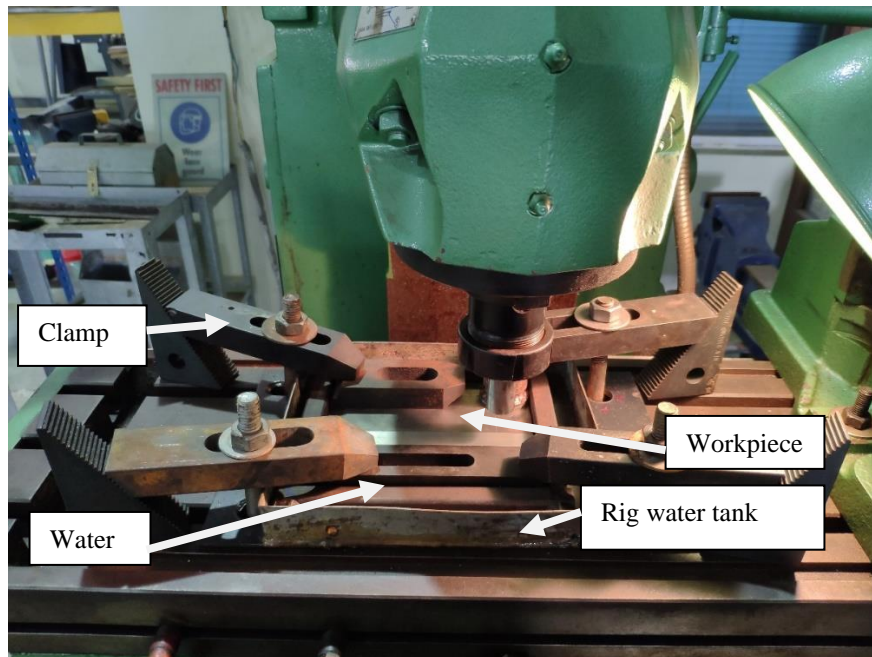


Figure 1: Experimental setup of FSW of butt joint between AA5083 and AA6061-T6 in the water environment.

Table 1 shows the chemical composition of the base material used to fabricate the joints. New specimens are employed with the total water immersed in a container to construct a butt-welded configuration during the technique.

Table 1: The chemical composition of aluminum alloy, reproduced from [25,26].

Weight (%)	Si	Fe	Cu	Mn	Mg	Zn	Ti
AA6061-T6	0.6	0.34	0.26	0.07	0.8	0.01	0.01
AA5083	0.40	0.40	0.1	0.2	0.4	0.1	0.15

Figure 2 shows the various tool pin profiles made of H13 high-speed steel, which included a cylindrical straight (C.S.), cylindrical threaded (C.T.), and tapered cylinder (T.C.) of 20 mm diameter shoulder and a diameter pin 7.2 mm; 4mm length.

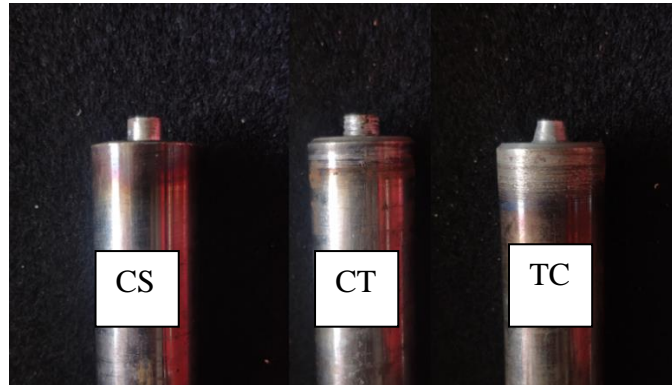


Figure 2: Different experimental tool pin profile

In the current experimental investigation, Table 2 displays a level process parameter. After fabricating the joint, take a tiny cross-section of each sample. The macrostructure profile assessed the joints; the welding condition was polished and etched in 10 to 30 seconds using a reagent containing methanol (25ml), nitric acid (25ml), hydrochloric acid (25ml), hydrofluoric acid (1 Drop) and inspected under an optical microscope. Vickers hardness testing was also performed on welded joints using a hardness machine with a force of 10kgf and a dwell period of 15s along the perpendicular to the cross-section.

Table 2: The level process of parameters

Parameters	Notation	Levels of factors		
		1	2	3
Speed	RPM	600	900	1200
Feed	Mm/min	30	60	90
Type of tool pin profile	TTPP	CS	CT	TC

2.1 Theory of Experimental Design

The experiment was conducted under the parametric design technique as per the Taguchi concept, which is an excellent approach for identifying relevant factors from many factors with a small number of tests. With nine rows corresponding to the number of tests and four columns at three levels. The experiment plan consists of 9 tests, with the first column representing the number of experiments run, the second column representing speed (rpm), the third column representing feed (mm/min), the fourth column representing pin profiles, and the fifth column representing hardness value, as shown in Table 3. The tests are replicated once for nine samples and allow for analysis of variance and signal to noise ratio, which displays the components evaluated and tabulated of the relevant levels.

Table 3: Experimental matrix

Experimental Run	Speed	Feed	Pin	Hardness
1	600	30	CS	75
2	600	60	CT	70
3	600	90	TC	73
4	900	30	CT	68
5	900	60	TC	72
6	900	90	CS	65
7	1200	30	TC	75
8	1200	60	CS	74
9	1200	90	CT	63

The experimental method investigates the effect of speed and feeds on joint strength properties and hardness under different tool pin profiles of the underwater friction stir welded joints. A Taguchi L9-orthogonal was used to examine the influence of the three variable factors. Each of the three parameters in the Taguchi statistical design has three levels. Three tool speeds (600, 900, and 1200 RPM) and three feed (30, 60, and 90 mm/min) were used for welds at varying levels, resulting in nine experimental samples. Each of the nine experimental samples has one replicates. With three levels of each factor, there are now points in the middle that allows for a curved fit response function. The design used is shown below in Table 2 and Figure. 7. This design allowed for an economical investigation into the cause-and-effect relationships of the two variables' significance.

3.0 RESULTS AND DISCUSSION

3.1 Welding Line Characteristics

Figure 3 shows the top surface appearances of underwater friction stir welded joints made of AA5083 and AA6061-T6 under various welding circumstances. The stirring behaviour appears to be consistent with the process parameter seen in the material deformation flow. However, in the final area of the joint, there are flashes with an undesirable appearance surface keyhole between the thermoplastic material (AA6061-T6). In addition, significant changes in ripple pattern and surface roughness were discovered in the C.S, CT, and T.C. pin profiles compared when rotational and transverse speeds. In these conditions, onion rings form prominently in the cross-sectional area.







Tool pin profile	Welding line	The cross-sectional joint of welded joint	Observation
Cylindrical straight			Tunnel defect at the mid thickness and insufficient heat input
Cylindrical threaded			Tunnel defect at the mid thickness and insufficient heat input
Tapered cylinder			Tunnel defect at the mid thickness and insufficient heat input

Figure 3: Macrograph of joint cross-section

The current study looks at the impact of a flat surface tool shoulder on heat generation. For all cases where the material stirring assumed enough penetration depth below the shoulder, joints generated no grooves on the surface of the weld site. Next, check if the weldment design at rotational tool and welding speed is considered a better weld line. They are owing to faster spinning speed, shearing the edge surface shoulder on the weld advancing side. As a result, there are a few flashes and the crowns at the weldment joints are harsher. The tool shoulder design's concave shoulder, on the other hand, is favoured because it offers the crown a smooth look and minimises unsightly flashing [14].

An experimental sample runs for a tapered cylinder pin profile with continuous rotating speeds of 900 rpm and welding rates of 60 mm/min are chosen for the inquiry. Figure 4 depicts the cross-sectional area under macrostructure observation. The characteristics of the aluminium joints were shown using a compound microscope, and image processing software was used to explain the grain structure at surface cross-sections. Figure 5 depicts a 5X, and 20X magnification picture of the stir zone and TMAZ region welded of tapered cylinder pin profile on AA5083 and AA6061-T6 joints, respectively. The microstructure of the composition of black dots is characterised using grain precipitation of aluminium in UFSW welded joints (Mg₂Si). The fluctuation in heat input distribution in the corresponding joint is related to material flow-induced inhomogeneous deformation along the weld line, which causes the creation of these phases.

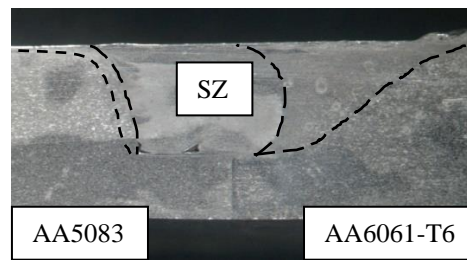


Figure 4: Cross-sectional area of sample 5 (900rpm and 60 mm/min)

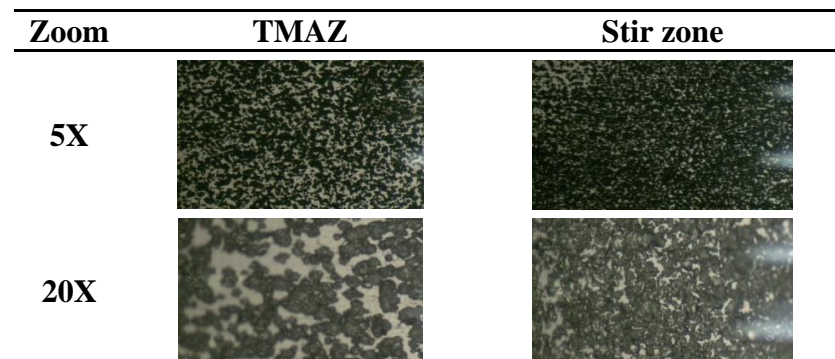


Figure 5: Magnification image at 900 rpm and 60mm/min

Figure 6 a) shows an onion ring layering formed when the materials are well mixed in the weld nugget. The banded structure (white circle) predominately influences the material flow and uniform mixing during FSW. The onion ring indicates that the stirring effect of the pin profiles under consistent welding speed at 60 mm/min is homogenous. Penetration of the material flow also provides critically adequate tool force and affects the quality of the connections distributed in the welding area. Dwell time significantly impacted temperature variations; otherwise, insufficient heat was generated due to fast welding speed and low joint strength, resulting in void defects on the advancing side (Figure 6 b).

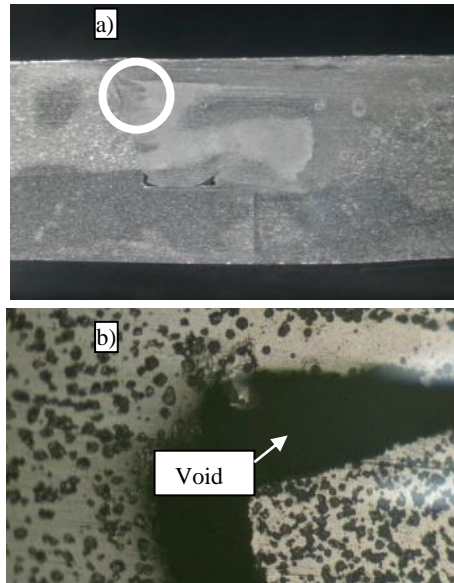


Figure 6: Cross-section of the joint created at a) material flow at advancing side and b) void defect at advancing side.

3.2 Effect of Water Environment on Hardness

In the current study, the rapid cooling rate is related to grain size, determined by water environment conditions. Due to this, there was inadequate time for grains to germinate in the soft zone, yet HAZ was reduced considerably. Weldment conditions are highly desired when the HAZ area is small. Rapid cooling minimises HAZ in soft places while increasing the hardness value on both sides of the welded connection. As a result, the strength of the joints, which are critical during the consolidation stage, is greatly affected. Furthermore, the intermediate heat input caused by underwater FSW bonds the metal, resulting in grain refinement and the prevention of coarse precipitation in the microstructure [26]. As a result, the water environment enhances hardness variation and keeps the best welded joint samples at temperatures above room temperature. Figure 7 shows both hardness profiles, with an unsymmetrical trend due to differences in physical parent material, particularly in the stir zone, which consists of dissimilar joints on advancing and retreating sides. The minimum hardness value in the dissimilar joint grows when the welding speed increases to the intermediate value with a high rotating speed. The profile plot of a tapered cylinder pin was profiled at the weld nugget zone at 900 rpm and a 60 mm/min feed rate. It displays the softening behaviour because of heat production during FSW at increasing rotational speeds.

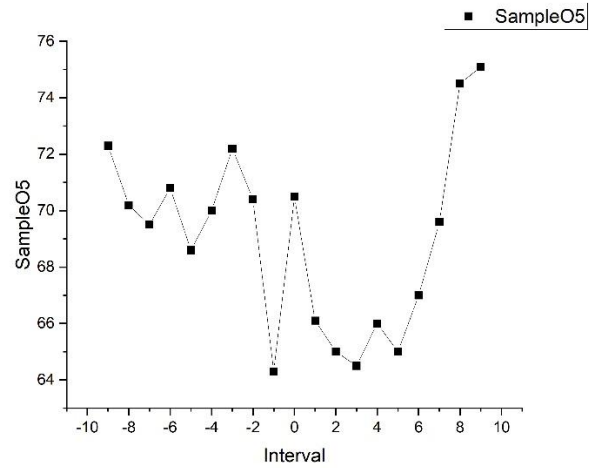


Figure 7: Hardness for tapered cylinder (900rpm and 60 mm/min)

Furthermore, the alloying placement should be considered so that all positions in the dissimilar welding joints have a higher hardness value. However, because it is close to the middle part of the weld, the front part of the AA5083 has an increasing hardness value. The rotational tool triggered the increasing hardness value, and the tapered cylinder pin provided suitable stirring at all welding speeds. The maximum hardness is 75Hv at 30mm/min. The lowest welding speed corresponds to the maximum hardness because the combined material, in turn, results in proper heat production during the welding process.

Tabulate data for hardness value; both cylindrical straight and tapered cylinder pin profiles have a higher hardness value than cylindrical threaded in the stir zone, as shown in Table 4. According to the optimal welding parameters found so far, the rotational tool speed was 900 rpm, and the welding speed was 60mm/min. The hardness distribution, which is highly impacted by water due to cooling agent changes in the microstructure, is a crucial issue in the welding zone. A softening region identified the lowest hardness under the pin throughout the stir zone, which was more pronounced in the thermos-mechanically affected zone (TMAZ) regions where the production process of observed tunnel defects was discovered.

Table 4: Summary data for hardness value

Experimental Run	Speed	Feed	Pin	Hardness
1	600	30	CS	75
2	600	60	CT	70
3	600	90	TC	73
4	900	30	CT	68
5	900	60	TC	72
6	900	90	CS	65
7	1200	30	TC	75
8	1200	60	CS	74
9	1200	90	CT	63
Average				71

3.3 Effect of Water Environment on Microstructure

The water in the rig container reduced heat regeneration, increased cooling rate, and aided grain microstructure refinement in the weld zone. At optimal temperatures, the temperature distribution identified the cooling action required to keep the stirring zone from overheating and enhance the recrystallisation microstructure in the weld nugget. The effect of underwater FSW, grain refining significantly influences water based on microstructural conditions [27]. With the content of this alloying element, joint strength boosted properties by the effect of the water environment [28]. Rapid cooling can generate a finer grain microstructure in the stir zone through lower treatment temperatures. The impact of the water depth on material cooling at greater tool rotational speed can be related to their mechanical characteristics and chemical composition [29]. However, the mechanical mixing of materials adds to excessive plastic deformation caused by designed tool movement.

3.4 Effect of Water Environment on Tool Pin Profile

The material mixing behaviour controls the significant effect of tool pin profile and welding speed in the welding junction underwater environment and grain refinement process. This condition was used on various pin profiles, and greater thermal dissipation reduces welding temperature. These advantages for process cooling rate produce fine microstructure, which increases weld durability and strength. However, the combination of process parameters is significantly influenced by plastic deformations, which creates excessive stirring from variances of tool pin profiles. In addition, because of the non-uniform material flow among the different materials, substantial volume defects such as tunnels and voids are formed due to incorrect mixing, and the softer material tends to extrude out of the nugget zone. Furthermore, because of its extensive circulation and extraordinary heat absorption capability, the water environment method has been explored to have a cooling effect on the samples during the welding process.

3.5 Analysis of Hardness

The analysis of variance approach is used to analyse and determine the statistically significant process parameters. At optimal process settings, mean and S/N ratio analysis for each of nine experimental units yields better joint strength results. Minitab 19 was used to generate the hardness values shown in Table 5.

Table 5: Summary of hardness experimental matrix data

Experimental Run	Speed	Feed	Pin	Hardness	S/N ratios (dB)	Hardness mean value
1	600	30	CS	75	37.5012	75
2	600	60	CT	70	36.9020	70
3	600	90	TC	73	37.2665	73
4	900	30	CT	68	36.6502	68
5	900	60	TC	72	37.1466	72
6	900	90	CS	65	36.2583	65
7	1200	30	TC	75	37.5012	75
8	1200	60	CS	74	37.3846	74
9	1200	90	CT	63	35.9868	63
Average				71		71

The ANOVA established a link between three process parameters and hardness for AA5083 and AA6061-T6 under variation of average S/N ratios and average hardness.

Tables 6 and 7 show the ANOVA analysis results for the S/N data and means of experiments. For the results, the third level of tool pin profile (tapered cylinder), the first level of welding speed (30 mm/min), and the first level of tool rotational speed (600 rpm) had the highest interaction reactions. Therefore, the hardness distribution value is advantageous for the pin profile, feed, and speed. R^2 values of 0.9640 and 0.9610 show that R^2 (adj) has a solid agreement of 0.8559 and 0.8440, respectively. Therefore, the effect of the welding parameter on the S/N ratio is the best level for the optimum hardness of the welded joints.

Table 6: Analysis of variance for means

Source	DF	Seq SS	Adj SS	Adj MS	F	P
Speed	2	28.222	28.222	14.111	5.08	0.164
Feed	2	57.556	57.556	28.778	10.36	0.088
Pin	2	62.889	62.889	31.444	11.32	0.081
Residual Error	2	5.556	5.556	2.778		
Total	8	154.222				

Model Summary

<i>S</i>	<i>R-Sq</i>	<i>R-Sq(adj)</i>
1.6667	96.40%	85.59%

Table 7: Analysis of Variance for SN ratios

Source	DF	Seq SS	Adj SS	Adj MS	F	P
Speed	2	0.43448	0.43448	0.21724	4.58	0.179
Feed	2	0.92504	0.92504	0.46252	9.74	0.093
Pin	2	0.97914	0.97914	0.48957	10.31	0.088
Residual Error	2	0.09494	0.09494	0.04747		
Total	8	2.43360				

Model Summary

<i>S</i>	<i>R-Sq</i>	<i>R-Sq(adj)</i>
0.2179	96.10%	84.40%

The Taguchi method was followed for the experimental runs. The average signal noise (S/N) ratios and mean values under various parameters at all three levels. Table 8 shows the estimated values of the response table for (S/N) ratios and the response table for means values for the nine experimental runs. A larger delta value suggests the parameter is more significant in affecting the response. Tool pin profile has been assigned a rank 1 in the response table, indicating it is the most influential parameter in influencing the response of experimental run, following welding speed (feed) and rotational speed. However, the ANOVA results for S/N and the mean of hardness were insignificant when under the process parameter of rotational speed. As a result, the general linear model (GLM) version of Transformed Response was used to describe the relevance of process factors in determining hardness within the stirred zone.

Table 8: Response table for the signal to noise ratios and means

Result	Response Table for Signal to Noise Ratios			Response Table for Means			
	Larger is Better						
Level	Speed	Feed	Pin	Level	Speed	Feed	Pin
1	37.22	37.22	37.05	1	72.67	72.67	71.33
2	36.69	37.14	36.51	2	68.33	72.00	67.00
3	36.96	36.50	37.30	3	70.67	67.00	73.33
Delta	0.54	0.71	0.79	Delta	4.33	5.67	6.33
Rank	3	2	1	Rank	3	2	1

Table 9 shows GLM ANOVA by determining analysis at different process parameters and the related hardness and calculating the percentage contribution of variables. Tool pin profiles and rotational speed types significantly impact model analysis using experimental parameters. All three variables revealed that the types of welding tools and welding speed are controlling the response. The tool pin profile has the largest contribution of such parameters: 41.45 percent and 31.33 percent feed, and 26.84 percent rotational speed. The software generates an estimated regression coefficients table for each response feature selected. In this case, the S/N ratio, and the mean two response characteristics were chosen for study. Use the p-values to identify statistically significant variables and the coefficients to compute the relative significance of each element in the model. As a significance threshold, any variables with p-values less than 0.05 are statistically significant. In this experimental approach, S/N ratios and mean are frequently utilised for model evaluation. Table 9 demonstrates that the general linear model transformed response is statistically significant at a mean level of 95 percent for tool pin profile ($p = 0.009$), welding speed ($p = 0.012$), and rotational speed ($p = 0.014$) at less than a mean level of 0.050. The rankings show that the tool pin profile affects the S/N ratio and the mean. The most significant influences on the S/N ratio and mean are rotational speed and welding speed, respectively.

Table 9: Analysis of Variance for Transformed Response

Source	DF	Seq SS	Contribution	Adj SS	Adj MS	F-Value	P-Value
SPEED	2	62.142	26.84%	62.1419	31.0710	71.25	0.014
FEED	2	72.551	31.33%	72.5510	36.2755	83.19	0.012
PIN	2	95.982	41.45%	95.9817	47.9909	110.06	0.009
Error	2	0.872	0.38%	0.8721	0.4361		
Total	8	231.547	100.00%				

The main effect plot for S/N ration and means response is used to find the best parameter combination. Figure 8 depicts a polar plot of the significant influence of welding parameters. The peak value shows the optimum result for main response of the S.N. ratio and means at each level, such as rotational speed and welding speed with various tool pin profiles. It is necessary to investigate welding conditions that match the hardness and give strength and pleasure to appearance. This crucial condition of weldment by heat generation along tool settings influenced such promised ineffectiveness by homogenising material flow shown to be significant in the welded zone.

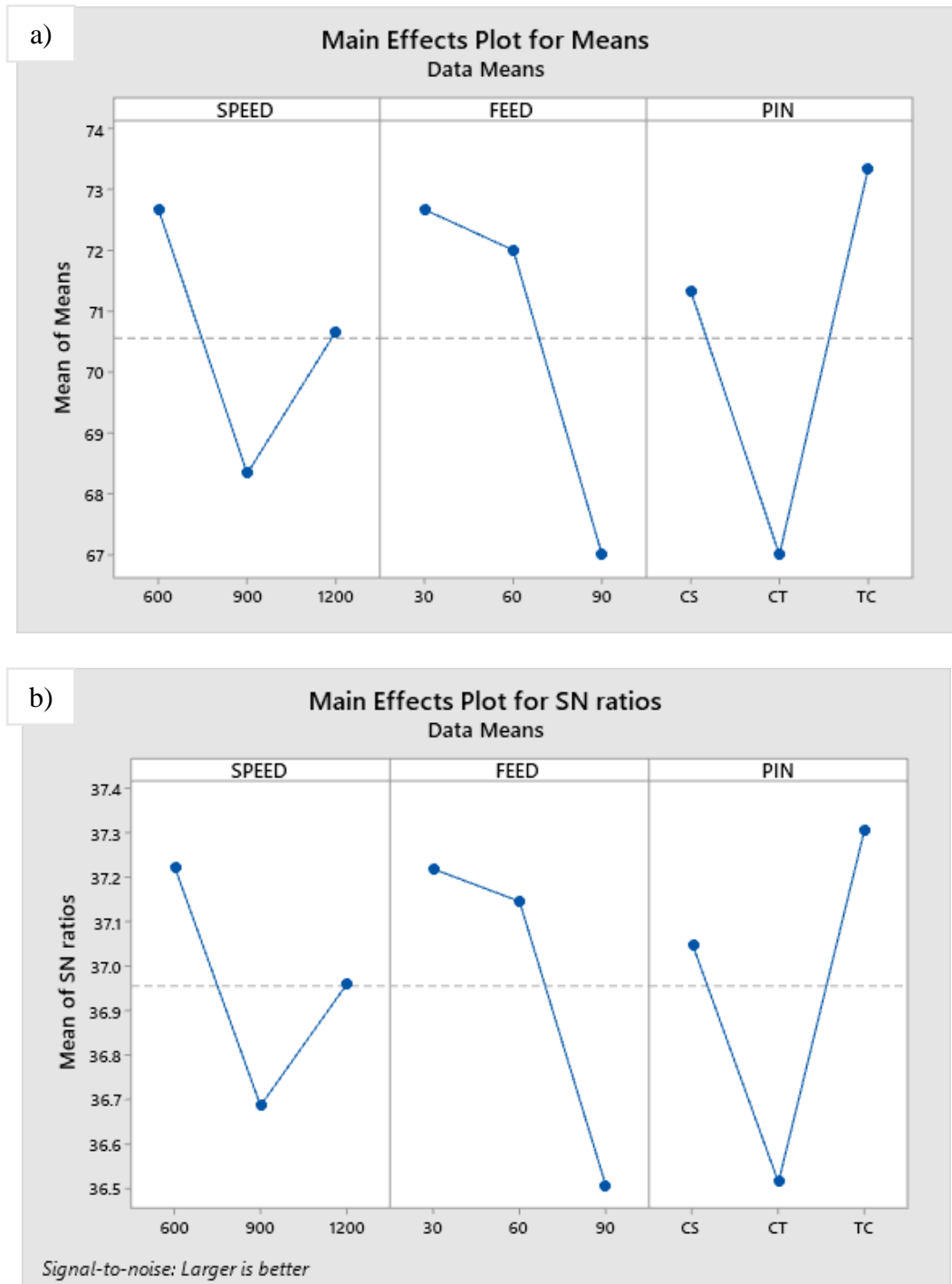


Figure 8: Main effect of welding parameters on hardness

Because this experiment aims to determine the best hardness value, the model was provided to forecast the hardness factor values that create the most significant mean of underwater FSW of AA5083 and AA6061-T6. As a result, the levels average in the response data below reveal that the welding parameter value for each factor correlates with the optimal level of all content following factor settings: rotational speed (600 rpm), welding speed (30 mm/min) and tool pin profile (tapered cylinder).

The experimental method has been validated by the significant impacts of welding settings on hardness value. Table 10 illustrates the best level for the highest hardness of welded joints when the tool pin profile is 77.56 HV under such conditions.

Table 10 Response to optimal conditions

Response	Prediction of the mean value	Average of the experimental value
Hardness (HV)	77.56	71

4.0 CONCLUSION

During underwater FSW of various AA5083 and AA6061-T6, parameters with hardness performance characteristics were optimised in this work. In friction stir welding, the underwater FSW technique was investigated in water cooling on different materials. The following is the result of the observation. First, there is a strong relationship between tool pin profile and welding speed (feed). In underwater friction stir welding, tapered cylinder tool profiles are the best tool pin profiles for AA5083 and AA6061-T6. Second, because heat concentration rises at the centreline and tool shoulder, the cooling medium assists in material churning beneath the pin tool. Third, the mixed zone's feed rate and tool rotation substantially influence the dissimilar materials in AA5083 and AA6061-T6 joints. Higher rotational speed results in less material mixing and help to achieve the degree banded structure mixing pattern. Fourth, stirring activity around the stir zone at varied welding conditions produces equiaxed grain, which substantially influences the microstructural properties of the joints. Finally, research has shown that the welding zone of retreating sides has a higher hardness than the advancing sides due to grain refinement and the cooling capabilities of the submerged environment. The data were subjected to an ANOVA analysis and a normal probability plot to demonstrate that it originated from a normally distributed population.

ACKNOWLEDGMENTS

This material is based upon work supported by the Ministry of Higher Education (MOHE), Malaysia and the Research Management Centre of UTM for the financial support through the RUG funding R.J130000.7851.5F382.

REFERENCES

1. Aissani M., Gachi S. Boubenider F. and Benkedda Y., 2010. Design and Optimisation Of Friction Stir Welding Tool, *Materials and Manufacturing Processes.*, 25: 1199–1205.
2. Rao M.S., Kumar B.V.R. and Hussain M., 2017. Experimental Study On The Effect Of Welding Parameters and Tool Pin Profiles On The Is:65032 Aluminium Alloy Fsw Joints, *Materials Today: Proceedings.*, 4: 1394–1404.
3. Raj, A., Kumar, J.P., Rego, A.M. and Rout, I.S., 2021. Optimisation of friction stir welding parameters during joining of AA3103 and AA7075 aluminium alloys using Taguchi method. *Materials Today: Proceedings*, 46, pp.7733-7739.
4. Shunmugasundaram, M., Kumar, A.P., Sankar, L.P. and Sivasankar, S., 2020. Optimisation of process parameters of friction stir welded dissimilar AA6063 and AA5052 aluminum alloys by Taguchi technique. *Materials Today: Proceedings*, 27, pp.871-876.
5. Kumar, P.V. and Paranthaman, P., 2021. Friction stir welding process parametric optimisation of hybrid aluminium-bagasse ash-graphite composite by Taguchi approach. *Materials Today: Proceedings*, 37, pp.764-768.
6. Wahid M.A., Khan Z.A. and Siddiquee A.N., 2018. Review On Underwater Friction Stir Welding: A Variant Of Friction Stir Welding With Great Potential Of Improving Joint Properties, *Transactions Of Nonferrous Metals Society Of China (English Edition).*, 28(2):193–219.
7. Liu G., Murr L.E., Niou C.S., McClure J.C. and Vega F.R. 1997. Microstructural Aspects Of The Friction-Stir Welding Of 6061-T6 Aluminium, *Scripta Materialia.*, 37: 355–361.
8. Baeslack W. A., Jata K. V. and Lienert T. J., 2006. Structure, Properties and Fracture Of Friction Stir Welds In A High-Temperature Al-8.5fe-1.3v-1.7si Alloy (Aa-8009), *Journal Of Materials Science.*, 41(10): 2939–2951.
9. Sakurada D., Katoh K. and H. Tokisue., 2002. Underwater Friction Welding Of 6061 Aluminium Alloy, *Journal Of Japan Institute Of Light Metals.*, 52(1): 2–6.
10. Bayazid S.M., Heddad M.M., and Cayiroglu I., 2018. A Review On Friction Stir Welding, Parameters, Microstructure, Mechanical Properties, Post-Weld Heat Treatment and Defects, *Material Science & Engineering International Journal.*, 2.
11. Mofid M.A., Abdollah Z.A., Ghaini F.M. and Gür C.H., 2012. Submerged Friction-Stir Welding (Sfsw) Underwater and Under Liquid Nitrogen: An Improved Method To Join Al Alloys To M.G. Alloys, *Metallurgical and Materials Transactions A.*, 43: 5106–5114.
12. Tan Y.B., Wang X.M., Ma M., Zhang J.X., Liu W.C., Fu R.D., and Xiang S., 2017. A Study On Microstructure and Mechanical Properties Of Aa 3003 Aluminium Alloy Joints By Underwater Friction Stir Welding, *Materials Characterization.*, 127: 41–52.
13. Sivachidambaram S. S., Rajamurugan G., Amirtharaj. and Divya., 2015. Optimising The Parameters For Friction Stir Welding Of Dissimilar Aluminium Alloys Aa 5383/Aa 7075, *Arpn Journal Of Engineering and Applied Sciences.*, 10: 5434–5437.
14. Palanivel R., Mathews P. K., Murugan N. and Dinaharan I., 2012. Effect Of Tool Rotational Speed and Pin Profile On Microstructure and Tensile Strength Of Dissimilar Friction Stir Welded Aa5083-H111 and Aa6351-T6 Aluminium Alloys, *Materials & Design.*, 40: 7–16.
15. Pietrusiewicz P., Błoch K., Nabiałek M. and Walters S. 2015. Influence Of 1% Addition Of N.B. and W On The Relaxation Process In Classical Fe-Based Amorphous Alloys, *Acta Physica Polonica A.*, 127: 397–399.
16. Nabiałek M., 2016. Influence Of The Quenching Rate On The Structure and Magnetic Properties Of The Fe-Based Amorphous Alloy, *Archives Of Metallurgy and Materials.*, 61: 439–444.
17. Gan W., Okamoto K., Hirano S., Chung K., Kim C. and Wagoner R.H., 2008. Properties Of Friction-Stir Welded Aluminium Alloys 6111 and 5083, *Journal Of Engineering Materials and Technology.*, 130.
18. Khodir S.A. and Shibayanagi T., 2008. Friction Stir Welding Of Dissimilar Aa2024 and Aa7075 Aluminium Alloys, *Materials Science and Engineering: B.*, 148: 82–87.
19. Emamikhah A., Abbasi A., Atefat A. and Givi M.K., 2013. Effect Of Tool Pin Profile On Friction Stir Butt Welding Of High-Zinc Brass (CuZn40), *The International Journal Of Advanced Manufacturing Technology.*, 71: 81–90.
20. Kovács Z. and Hareancz F., 2018. Joining Of Non-Weldable Aa7075 and Weldable Aa6082 Aluminium Alloy Sheets By Friction Stir Welding, *Iop Conference Series: Materials Science and Engineering.*, 448(012001).
21. Hamed J. A., 2017. Effect Of Welding Heat Input and Post-Weld Ageing Time On Microstructure and Mechanical Properties In Dissimilar Friction Stir Welded Aa7075aa5086, *Trans. Nonferrous Met. Soc. China.*, 27: 1707-1715.
22. Xu W.F., Liu J.H., Chen D.L., Luan G.H. and Yao J.S., 2012. Improvements Of Strength and Ductility In Aluminium Alloy Joints Via Rapid Cooling During Friction Stir Welding, *Materials Science and Engineering: A.*, 548: 89–98.
23. Heidarzadeh A., Mironov S., Kaibyshev R., Çam G., Simar A., Gerlich A., 2021. Friction Stir Welding/Processing Of Metals and Alloys: A Comprehensive Review On Microstructural Evolution, *Progress In Materials Science.*, 117 (100752).
24. Khodir S.A. and Shibayanagi T., 2008. Friction Stir Welding Of Dissimilar Aa2024 and Aa7075 Aluminium Alloys, *Materials Science and Engineering: B.*, 148: 82–87.
25. Hasan M., Abdi R. and Akbari M., 2013. Modelling and Pareto Optimisation Of Mechanical Properties Of Friction Stir Welded AA7075 / AA5083 Butt Joints Using Neural Network and Particle Swarm Algorithm, *Materials and Design.*, 44: 190–198.
26. Fathi J., Ebrahimzadeh P., Farasati R. and Teimouri R., 2019. Friction Stir Welding Of Aluminium 6061-T6 In Presence Of Water-Cooling: Analysing Mechanical Properties and Residual Stress Distribution, *International Journal Of Lightweight Materials and Manufacture.*, 2: 107–115.
27. Shanavas S., Dhas J.E.R. and Murugan N., 2018. Weldability Of Marine Grade AA 5052 Aluminium Alloy By Underwater Friction Stir Welding, *The International Journal Of Advanced Manufacturing Technology.*, 95: 4535–4546.
28. Yoon J., Kim C., and Rhee S., 2019. Performance Of Plunge Depth Control Methods During Friction Stir Welding, *Metals.*, 9(283).
29. Nabiałek M., Pietrusiewicz P., Dośpiał M., Szota M., Gondro J., Gruszka K., 2014. Influence Of The Cooling Speed On The Soft Magnetic and Mechanical Properties Of FE61CO10Y8W1B20 Amorphous Alloy, *Journal Of Alloys and Compounds.*, 615: 56-60.